Accepted Manuscript

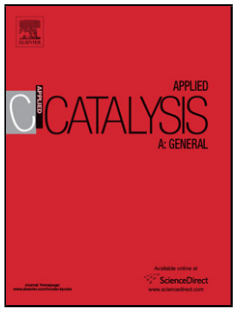

Title: Platinum nanoparticles onto pegylated poly(lactic acid) stereocomplex for highly selective hydrogenation of aromatic nitrocompounds to anilines

Authors: Werner Oberhauser, Claudio Evangelisti, Cristina Tiozzo, Mattia Bartoli, Marco Frediani, Elisa Passaglia, Luca Rosi

PII: S0926-860X(17)30092-3
DOI: http://dx.doi.org/doi:10.1016/j.apcata.2017.03.003
Reference: APCATA 16162

To appear in: *Applied Catalysis A: General*

Received date: 4-1-2017
Revised date: 28-2-2017
Accepted date: 2-3-2017

Please cite this article as: Werner Oberhauser, Claudio Evangelisti, Cristina Tiozzo, Mattia Bartoli, Marco Frediani, Elisa Passaglia, Luca Rosi, Platinum nanoparticles onto pegylated poly(lactic acid) stereocomplex for highly selective hydrogenation of aromatic nitrocompounds to anilines, Applied Catalysis A, General http://dx.doi.org/10.1016/j.apcata.2017.03.003

Platinum nanoparticles onto pegylated poly(lactic acid) stereocomplex for highly selective hydrogenation of aromatic nitrocompounds to anilines

Werner Oberhauser [a,*], Claudio Evangelisti [b,*], Cristina Tiozzo [b], Mattia Bartoli [c], Marco Frediani [c], Elisa Passaglia [d], Luca Rosi [c]

[a] *Istituto di Chimica dei Composti Organometallici (CNR-ICCOM), 50019 Sesto Fiorentino, Italy*

[b] *Istituto di Scienze e Tecnologie Molecolari (CNR-ISTM), 20138 Milano, Italy*

[c] *Dipartimento di Chimica, Università Degli Studi di Firenze, via della Lastruccia 13, 50019 Sesto Fiorentino, Italy*

[d] *CNR-ICCOM, UOS Pisa, Area della Ricerca, via Moruzzi 1, 56124 Pisa, Italy*

*Corresponding authors. E-mail addresses: werner.oberhauser@iccom.cnr.it (W. Oberhauser), claudio.evangelisti@istm.cnr.it (C. Evangelisti)

Graphical abstract

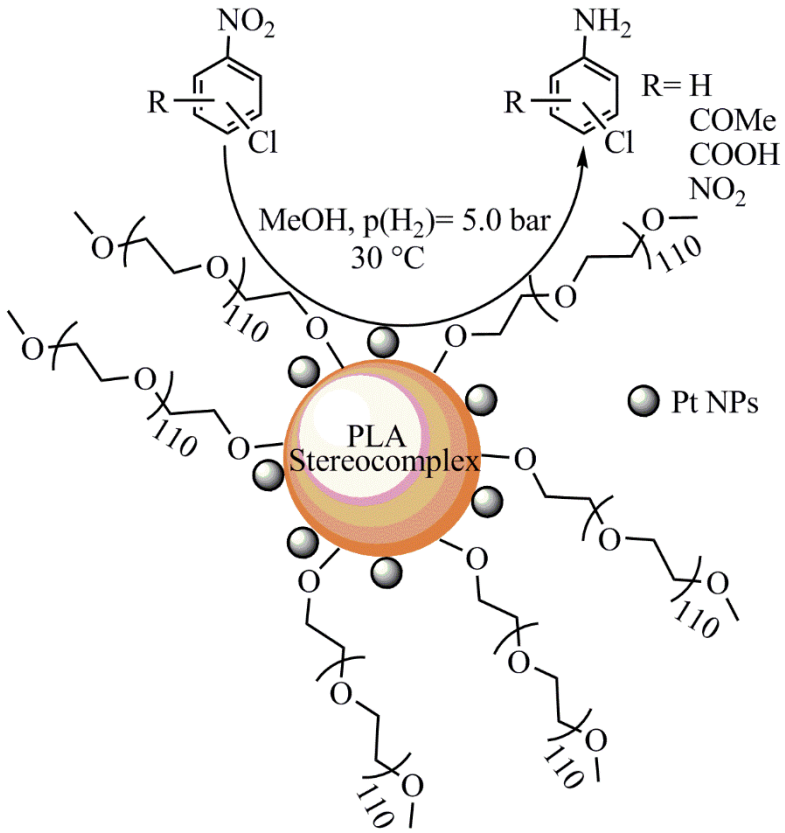

Highlights

- Pegylated poly(lactic acid) stereocomplex (L) was stable in methanol at room temperature.
- Pt nanoparticles on L hydrogenated aromatic nitrocompounds to anilines.
- Covalently attached polyethyleneglycol contributed to catalytic activity.
- The high chemoselectivity for anilines was Pt nanoparticles' size-dependent.

ABSTRACT

A stereocomplexed poly(lactic acid)-polyethyleneglycol copolymer was synthesized and successfully used as recyclable support for Pt nanoparticles, generated by the metal vapor synthesis technique. The confinement of the Pt nanoparticles were determined by thermal analysis. Hydrogenation reactions of chlorinated aromatic nitro compounds, containing other reducible functional groups, to the corresponding anilines occurred with the latter supported Pt nanoparticles in MeOH under very mild reaction conditions (*i.e.* 30 °C, $p(H_2)$= 5.0 bar). The covalently attached polyethyleneglycol polymer significantly increased the catalytic activity of the supported Pt nanoparticles compared to an analogous catalytic system which did not contain polyethyleneglycol but the same sized Pt nanoparticles.

Keywords: Poly(lactic acid)/Platinum/Hydrogenation/Aromatic Nitrocompounds

1. Introduction

Hydrogenation of nitro arenes to the corresponding aniline is a chemical transformation of remarkable interest, due to application of anilines as intermediates for the industrial production of polymers, agrochemicals, dyes and pharmaceuticals [1]. The hydrogenation of nitroarenes that contain also other reducible functional groups and halide atoms is especially challenging, since reduction of second functional group and dehalogenation reactions can occur [2]. In addition the hydrogenation of the nitro group itself can led to various interesting intermediates such as hydroxylamines [3,4]. In order to make this hydrogenation reaction sustainable various supported metal nanoparticles (NPs) of Pd [5-7], Ni [8], Ru [9], Ag [10,11], Fe [12], Au [13,14] and Pt [15,16] were used. Pt NPs-mediated nitro compound hydrogenation reactions are generally chemoselective for the corresponding aniline, applying very mild reaction conditions (*i.e.* < 40 °C,

p(H_2)= 5.0 bar, MeOH) [2]. The undesired dehalogenation reaction of aromatic nitro compounds was decreased significantly by supporting Pt-NPs onto partially reduced γ-Fe_2O_3, decreasing the electron back-donation from d orbitals of Pt to the π* anti-orbitals of the adsorbed molecules [17-19]. High chemoselectivity for the conversion of nitro arenes to anilines has been obtained with sol-gel encapsulated [20], porous polymeric framework confined [21-23], ionic polymer-[24] and ionic liquids-stabilized NPs [25,26]. Remarkable results have also been reported for polyethylene glycol (PEG)-stabilized Pt-NPs in methanol [27] and supercritical CO_2 [28]. PEG has unique applications in metal-mediated transformations as reaction medium, to stabilize heterogeneous catalysts and as phase transfer catalyst [2,29]. Recently we introduced stereocomplexed (sc) poly(lactic acid) (PLA) as a new biodegradable support for Pd-catalyzed selective hydrogenation reactions [30,31]. Herein we report the synthesis and application of a sc-PLA-PEG block copolymer [32] as new recyclable polymer support for chemoselective, Pt-NP-mediated hydrogenation reactions of aromatic Chloro-nitro compounds to the corresponding aniline in MeOH.

2. Experimental

2.1. Materials

Tin octanoate ($Sn(Oct)_2$), benzylalcohol, polyethyleneglycol monomethylether (PEG 5000, M_n= 4870 g/mol, polydispersity index (PDI)= 1.20) and *l*-and *d*-lactide were purchased from Aldrich. *L*- and *d*-lactide were sublimated before utilization and stored thereafter under nitrogen atmosphere at 4.0 °C. All operations involving the metal vapor synthesis (MVS) products were performed under a dry argon atmosphere. Mesitylene was purchased from Aldrich and purified by conventional methods, distilled and stored under argon. Ketjenblack EC-600JD (C) was purchased from Cabot Corp. USA, while solvents such as *n*-hexane, CH_2Cl_2, CH_3OH, $CDCl_3$, CD_3OD and HPLC-grade THF were purchased from Aldrich and used without further purification.

2.2. Instruments

^{1}H and $^{13}C\{^{1}H\}$ NMR spectra were recorded on a Bruker Avance 400 spectrometer, measuring at 400.13 and 100.62 MHz.

ATR-IR spectra were recorded on a Shimadzu model IR-Affinity apparatus, equipped with a Golden Gate single reflection diamond ATR accessory.

Gel-Permeation Chromatography (GPC) was carried out with a Waters Binary HPLC 1525 pump, a manual injector with a six way valve and a 200 μL loop, three in series connected Shodex KF-802, KF-803 and KF-804 columns (length: 300 mm each, inner diameter: 8.0 mm, 24500 theoretical plates, exclusion limit for polystyrene (PS) up to 400000 g mol^{-1}; a refraction index (RI) detector (Optilab T-rEXTM, Wyatt Technology) and a UV detector (Waters mod. 2489). HPLC-grade THF with a water content of maximal 0.1 vol% was used as eluent at a constant flow of 1.0 mL min^{-1}, keeping the columns at 30.0 °C with a thermostat. The GPC system was calibrated using PS as standard. Samples were prepared by dissolving 5.0 mg of analyte in 1.0 mL of eluent. The obtained solution was filtered through a 0.2 μm PTFE filter and injected.

GC analyses were performed with a Shimadzu 2010 gaschromatograph equipped with a flame ionization detector and a 30.0 m (0.25 mm i.d., 0.25 μm film thickness) VF-WAXms capillary column.

GC-MS analyses were performed with a Shimadzu QP5000 apparatus, equipped with a 30 m (0.32 mm i.d., 0.50 μm film thickness) CP-WAX 52CB WCOT-fused silica column.

High resolution transmission electron microscopy (HRTEM) analyses of the supported Pt-NPs was carried out with a ZEISS LIBRA 200FE HRTEM instrument, equipped with a FEG source operating at 200.0 kV, in column second-generation omega filter for energy selective spectroscopy

(EELS) and imaging (ESI), HAADF STEM facility, EDS probe for chemical analysis, integrated tomographic HW and SW. The samples were ultrasonically dissolved in a 1:1 solvent mixture of isopropanol/$CHCl_3$ and a drop of the obtained solution was deposited on a holey-carbon film supported on a copper TEM grid of 300 mesh. Histograms of the particle size distribution were obtained by counting at least 500 particles. The mean particle diameter (d_m) was calculated by using the formula $d_m = \sum d_i n_i / \sum n_i$, where n_i is the number of particles with diameter d_i.

Inductively coupled plasma-optical emission spectrometry (ICP-OES) was carried out with an iCAP 6200 Duo upgrade, Thermofisher instrument. A sample (0.5 mL) of Pt-solvated metal atoms (SMA) solution was heated over a heating plate in a porcelain crucible in the presence of aqua regia (2.0 mL) for six times followed by dissolving the solid residue in 0.5 M aqueous HCl.

Powder X-ray diffraction (PXRD) experiments were carried out at room temperature with a PANalytical X'PERT PRO powder diffractometer, employing Cu K_α (λ = 1.5418 Å) radiation and a parabolic MPD-mirror.

Thermogravimetric (TG) analyses were carried out under nitrogen atmosphere using a Seiko, Parabiaco (Mi) Italy EXSTAR 7200 TG/DTA instrument. TG curves were collected on samples of 5-10.0 mg in the temperature range from 30.0 to 700.0 °C (N_2 flow = 200.0 mL/min) with a heating rate of 10.0 °C/min. The onset temperature of degradation (T_{onset}) is defined as the temperature that corresponds to the intercept of tangents to the curve before and after the degradation step. The maximum rate inflection temperature for the different degradation steps was extracted from derivative TG (DTG) curves.

Differential scanning calorimetry (DSC) analysis of all the samples was carried out under nitrogen atmosphere by using a Perkin-Elmer 4000 instrument. The instrument was calibrated with indium and lead as standards. The analysis was carried out in a temperature range depending on the thermal features of polymer blocks at 10.0 °C/min. As for example it was from -40.0 to 240.0 °C

for the stereoblock-based samples. Crystallization and melting enthalpies were evaluated from the integrated areas of melting peaks recorded during second heating.

Environmental scanning electron microscopy (ESEM) images for L^1 and L^2 were acquired on a FEI ESEM Quanta 200 apparatus with a tungsten source using a gaseous secondary electron detector (GSED) with a 500.0 μm aperture. The images were collected with a magnification of 3000x a chamber pressure of 3.0 Torr and a working distance of 7.0 mm.

2.3. Synthesis

2.3.1. Synthesis of l/d-PLA-Bn

In a Schlenk tube, *l*/*d*-lcatide (4.0 g, 28.0 mmol) was heated at 135.0 °C in the presence of $Sn(Oct)_2$ (56.3 mg, 0.139 mmol) and benzylalkohol (BnOH) (43.3 mg, 0.40 mmol) for 3 h under a nitrogen atmosphere. Then the reaction mixture was allowed to cool to room temperature and the sublimed crystalline lactide fraction (ca. 1.0 %) was removed mechanically from the Schlenk tube. The crude reaction product was dissolved in $CHCl_3$ (20.0 mL) and upon the slow addition of *n*-hexane (30.0 mL) to the latter solution the product precipitated as light pink powder. The solid was separated from solution by filtration, washed several times with *n*-hexane and dried by vacuum at room temperature for 12h. ^{1}H NMR data acquired of the product correspond to that reported in the literature [33].

Yield: *l*-PLA-Bn (3.8g, 95%); *d*-PLA-Bn (3.5 g, 88%); M_n: *l*-PLA-Bn (10240 g/mol), PDI (1.31); *d*-PLA-Bn (9240 g/mol), PDI (1.33).

2.3.2.Synthesis of l/d-PLA-PEG

In a two necked round bottom flask *l*/*d*-lactide (3.0 g, 21.0 mmol) was solubilized in anhydrous toluene (30.0 mL) and refluxed for 24h in the presence of $Sn(Oct)_2$ (35.18 mg, 0.087 mmol) and PEG monomethyl ether (3.0 mg, 0.60 mmol). During the reaction the product precipitated as white solid, which was isolated and dissolved in CH_2Cl_2 (15.0 mL). Upon addition of *n*-hexane (30.0 mL) to the latter solution the product precipitated as off-white powder, which was separated from solution by filtration, washed with *n*-hexane (10.0 mL) and dried under vacuum for 12h.

Yield: *l*-PLA-PEG (5.2g, 87%); *d*-PLA-PEG (5.6 g, 93%). M_n: *l*-PLA-PEG (8980 g/mol), PDI (1.38); *d*-PLA-PEG (9163 g/mol), PDI (1.48).

^{1}H NMR of *l*-PLA-PEG (400.13 MHz, $CDCl_3$, ppm) δ= 1.49 (d, $^3J_{HH}$= 7.2 Hz, 3H, CH_3(terminal)), 1.58 (d, $^3J_{HH}$= 7.1 Hz, 171H, CH_3), 3.39 (s, OCH_3), 3.47 (m, 2H, CH_2), 3.64 (s, 440H, CH_2), 4.38 (br. s, 1H, CH(terminal)), 5.15 (q, $^3J_{HH}$= 7.1 Hz, 57H, CH).

$^{13}C\{^1H\}$ NMR (100.62 MHz, $CDCl_3$, ppm) δ= 16.63 (s, CH_3), 20.51 (s, CH_3(terminal)), 58.99 (s, OCH3), 64.43 (s, OCH_2), 66.68 (s, CH(terminal)(PLA)), 69.00 (s, CH(PLA)), 70.54 (s, CH_2), 71.92 (s, CH_2O), 169.60 (s, *C*OOC), 175.10 (s, *C*OOC(terminal)).

2.3.3.Synthesis of L^1 and L^2

L-PLA-Bn (2.0 g) and *d*-PLA-Bn (2.0 g) were separately dissolved in CH_2Cl_2 (20.0 mL) and the resulting solutions combined at room temperature, followed by stirring for half an hour. Afterwards the solvent was completely evaporated and the off-white solid dried under vacuum at room temperature for 16h. The same synthetic procedure was applied for L^2, using *l*-PLA-PEG (2.0 g) and *d*-PLA-PEG (2.0 g).

Yield: L^1 (3.7 g, 93%); L^2 (3.8 g, 95%).

2.3.4.Synthesis of Pt@L^1/L^2/PEG/C

The Pt-NPs supported onto L^1, L^2, PEG and Carbon were synthesized using the metal vapor synthesis (MVS) technique as follows: Platinum vapors generated at 10^{-5} mbar by resistive heating of a tungsten wire surface coated with electrodeposited platinum (ca. 120.0 mg) were co-condensed with mesitylene (100.0 mL) at -196.0 °C in a glass reactor as described elsewhere [34]. The reactor chamber was heated to the melting point of the solid matrix and the resulting brown solution (95.0 mL) was kept under argon atmosphere in a Schlenk tube at -30/-40.0 °C. The Pt-content of the obtained Pt solvated metal atoms (SMA) was determined by ICP-OES (1.0 mg Pt / mL). In a 250.0 mL Schlenk tube L^1 (0.720 g) was suspended in CH_2Cl_2 (20.0 mL) and the solution was left in an ultrasonic bath for 30 minutes. Afterwards the Pt/mesitylene solution (7.0 mL, C_{Pt} = 1.0 mg/mL) was added to the suspension. The mixture was stirred overnight under inert atmosphere at room temperature. The day after the polymer was quantitatively precipitated with diethyl ether (100.0 mL) and the solid was dried under vacuum. The same synthetic procedure was used for L^2 (0.600 g), PEG (0.350 g) and C (0.600 g). The Pt metal loading on L^1, L^2, PEG and carbon-support was determined by ICP-OES, after microwave digestion (i.e. addition of HNO_3 65% (5.0 mL) + H_2O_2 30% (1.0 mL) and then aqua regia (3.0 mL) to the isolated catalyst (5.0 mg)). The obtained solution was diluted with highly deionized water to a final weight of 10.0 g. All catalysts contained 1.0 wt% of Pt.

2.4. Stability of L^2 in MeOH at room temperature and at 80.0 °C

L^2 (20.0 mg) was suspended in MeOH (0.5 mL) at room temperature and 10 drops of the resulting suspension were put in the cavity of a Si-wafer (zero background) followed by the acquisition of a PXRD spectrum at room temperature. For comparison reasons the PXRD spectrum of as-synthesized L^2 was acquired at the same temperature.

The stability of L^2 against transesterification reactions in methanol (*i.e.* reaction medium for the catalytic hydrogenation of aromatic nitro compounds) was proved by suspending L^2 in CD_3OD and heating the obtained suspension at 80.0 °C for 2h. Afterwards, the reaction temperature was decreased to room temperature and an ^1H NMR spectrum acquired. The methanol solution was further analyzed by GC-MS.

2.5. Catalytic hydrogenation reactions in MeOH

Pt@L^1/L^2/C (25.0 mg, 1.282 μmol of Pt) and the desired amount of substrate were placed in a Teflon-coated stainless steel autoclave (80.0 mL), equipped with magnetic stirrer, temperature and pressure controller. The autoclave was then sealed and evacuated, followed by charging it with deaerated MeOH (10.0 mL) by suction. Afterwards, the autoclave was placed in an oil path which was heated to 30.0 °C. Once the latter temperature was reached, the autoclave was pressurized with hydrogen (5.0 bar) and stirred at 800 rpm. After the desired reaction time, the autoclave was removed from the oil bath and cooled to 20.0 °C, followed by venting the excess hydrogen. The suspension was centrifuged and the catalytic solution separated from catalyst by decantation in air atmosphere. To the latter solutions *n*-dodecane (100.0 μL, 0.44 mmol) was added as external standard and analyzed by GC. Recycling experiments were conducted by using recovered Pt@$L^{1/2}$, applying the above descript protocol. The $Pt_{surface}$-atom related TOF (h^{-1}) values were calculated according to the following equation: mmol(converted substrate) × [mmol($Pt_{surface}$) × h]$^{-1}$. The mmol of $Pt_{surface}$ (*i.e.* amount of Pt atoms exposed to the substrate) using 25.0 mg of catalyst for the hydrogenation reactions were 0.7179 μmol for Pt@L^1 and 0.7948 μmol for Pt@L^2 and Pt@C, according to the percentage of Pt-atoms localized on the NPs' surface (*i.e.* 56% (Pt@L^1) and 62% for Pt@L^2/C), using a HRTEM-based calculation [35].

3. Results and discussion

The PLA-based support L^1 was synthesized, as previously reported [31], by a two step reaction (Scheme 1a) which comprised the ring opening polymerization (ROP) of *l*/*d*-lactide in bulk, using $Sn(Oct)_2$ as catalyst and benzyl alcohol (BnOH) as initiator molecule. Afterwards equimolar CH_2Cl_2 solutions of the obtained polymers, featured by an opposite stereochemistry (*i.e. l*-PLA-Bn and *d*-PLA-Bn), were reacted at room temperature and on evaporation of the solvent L^1 was obtained as off-white solid. The synthesis of L^2 differed from that of L^1 regarding the synthesis of the copolymers *l*/*d*-PLA-PEG (Scheme 1b), which occurred in refluxing toluene using PEG monomethylether (HO-PEG-OMe) as initiator molecule.

Sn(II) residue stemming from the ROP catalyst were always found in the final PLA-based supports as recently confirmed by XPS analysis [31].

The occurred formation of the PLA-PEG-OMe copolymers was proved by ^1H and $^{13}C\{^1H\}$ NMR spectroscopy. The $^{13}C\{^1H\}$ NMR singlet at 175.10 ppm, which was assigned to the terminal carboxylic ester group [31] confirmed the covalent bonding of PEG monomethyl ether to PLA.

In addition, GPC-analysis of isolated *l*- and *d*-PLA-PEG-OMe carried out in THF (Fig. S1) confirmed an increase of the molecular weight from 4870 g/mol (PEG) to around 9000 g/mol of the copolymers. DSC analysis, carried out with *l*-PLA-PEG-OMe showed two melting points at 54.9 and 135.5 °C, in agreement with the presence of a crystalline PEG and PLA phase, respectively (Table S1). The formation of L^2 was confirmed by PXRD and DSC analysis. Accordingly, the PXRD spectrum of L^2 (Fig. 1, trace c) showed as that of L^1 (Fig. 1, trace a) the presence of typical Bragg reflexes of sc-PLA centered at 11.89, 20.75 and 24.10 (shoulder) (2θ) and those of a crystalline PEG phase (Fig. 1, trace b).

DSC data for L^2 (Table S1) were in accordance with the presence of a PEG phase, showing a characteristic melting temperature at 57.7 °C and a second melting point at 208.2 °C (*i.e.* T_m of sc-PLA), which is slightly lower compared to what has been found for L^1 (*i.e.* 216.2 °C). In addition an ATIR spectrum of L^2 showed the presence of a strong C-O-C stretching band at 1089 cm^{-1}, which is characteristic for PEG (Fig. S2).

ESEM images of L^1 and L^2 (Fig. S3) confirmed a much rougher surface in L^1 compared to L^2, where the sc-PLA is covered by a PEG phase resulting a waxy-like surface. L^1-type stereocomplexes have shown a BET surface of ca. 150 m^2/g with a pore volume of 0.45 mL/g [36]. BET analysis of L^2 were not performed since the PEG phase melted during the surface cleaning step at 100.0 °C.

The stability of L^2 in MeOH (*i.e.* reaction medium of the catalytic aromatic nitro compound hydrogenation reactions) against stereoblock dissociation to *l*/*d*-PLA-PEG-OMe and occurring transesterfication reactions was proved by PXRD and ^{1}H NMR spectroscopy, respectively.

As a result, the PXRD spectrum of a MeOH suspension of L^2 (Fig. 2, trace b) showed clearly the presence of Bragg reflexes of sc-PLA, while Bragg reflexes assigned to PEG were not observed due to the solubility of PEG in MeOH.

Accordingly, the ^{1}H NMR spectrum of L^2, acquired in CD_3OD, showed only a singlet at 3.63 ppm for the CH_2 units of PEG (Fig. S4). The same ^{1}H NMR pattern at room temperature was observed after heating the latter solution at 80.0 °C for 2h (Fig. S3, trace c). In addition, GC-MS analysis carried out on the suspension after heating to 80.0 °C confirmed the absence of products stemming from transesterfication reactions.

$L^{1/2}$ were used to support Pt NPs, generated by metal vapor synthesis (MVS) technique, where Pt-clusters are generated and stabilized by an appropriate solvent [19,34]. The addition of a mesitylene solution of mesitylene-stabilized Pt NPs to a CH_2Cl_2 suspension of L^1 and L^2 followed by the addition of an excess of diethyl ether led to supported Pt NPs (*i.e.* Pt@L^1 and Pt@L^2) (Scheme 1c) as grey and black precipitate, respectively, with a Pt content of 1.0 wt%, as determined by ICP-OES. HRTEM analysis, of the supported Pt NPs (Fig. 3) showed particle sizes of 1.6 ± 0.5 and 1.4 ± 0.3 nm for Pt@L^1 and Pt@L^2, respectively.

In order to evaluate the stabilizing effect of PEG on Pt NPs, generated by the reported MVS technique, we treated the same mesitylene-stabilized Pt NPs, as used for the synthesis of Pt@L^1/L^2 with neat PEG, isolating Pt@PEG, featured by the same Pt content of 1.0 wt% (Scheme 1c). The corresponding HRTEM analysis showed the formation of significantly larger Pt NPs (Fig. S5) (2.4 ± 0.6 nm), indicating that the ether functionalities in the mobile PEG polymer chains have a lower stabilizing effect on Pt NPs [26] compared to the sc-PLA polymer. PXRD spectra of $L^{1/2}$ and Pt@$L^{1/2}$ (Fig. 4) proved the absence of significant polymer morphology alteration by applying the experimental conditions to $L^{1/2}$, necessary to support Pt NPs by the metal MVS technique.

In addition, a TG analysis of L^2, recovered after treating in the same way as described for the MVS technique (i.e. sonication of a CH_2Cl_2 suspension of L^2, followed by precipitation with diethyl ether), without supporting Pt-NPs, gave the same characteristic TG data as the as-synthesized L^2 (Table S2), confirming the absence of structural alterations of the copolymer by supporting Pt NPs onto it.

In order to study the confinement of the supported Pt NPs on L^2, we exploited the change of thermal behavior of PLA-based polymers in the presence of NPs, as observed for Pd NPs under related conditions [30,31].

To this purpose, we carried out DSC and TG analysis on Pt@$L^{1/2}$/PEG (Tables S1/2 and Figs. S8/9) in the presence of a nitrogen atmosphere.

DSC analysis of Pt@L^1 showed a significantly higher melting (T_m) and crystallization temperature (T_c) compared to L^1 (*i.e.* 228.5 *vs* 216.2 °C and 203.7 *vs* 188.8 °C) associated with higher enthalpies of the corresponding phase transition. In addition, TG profiles acquired under nitrogen notably exhibited an increase of the onset temperature of polymer degradation in the presence of Pt NPs (*i.e.* 285.8 °C (Pt@L^1) *vs* 236.7 °C (L^1)), as observed for Pd NPs on the same type of support [31]. DSC and TG data for the sc-PLA part of Pt@L^2 and L^2 followed the same trend as observed for Pt@L^1 and L^1, although less pronounced. In contrast, Pt NPs on PEG, which are larger in size compared to those on $L^{1/2}$ (*i.e.* 2.4 *vs* 1.6 and 1.4 nm, respectively), decreased T_m of PEG (*i.e* 59.9 °C (Pt@PEG) *vs* 62.4 °C (PEG)) and the polymer thermal stability (T_{onset}) compared to PEG (*i.e.* 340.7 °C (Pt@PEG) *vs* 384.3 °C (PEG)).

Experimental data obtained from thermal analyses and HRTEM measurements of Pt@$L^{1/2}$/PEG (Tables S1 and S2) were indicative for the confinement of Pt NPs on the sc-PLA part of L^2.

Pt@$L^{1/2}$ were employed to catalyze the selective hydrogenation of aromatic nitrocompounds to the corresponding anilines in MeOH, which is the solvent of choice for selective hydrogenation to anilines [2], at 30.0 °C and in the presence of hydrogen (5.0 bar). All substrates used for the catalytic screening contained a chlorine atom and some of them also a second reducible functional group as shown in Scheme 2.

Pt NPs supported onto Ketjenblack (Pt@C), which is a high surface carbonaceous support (S_{BET}= 1400 m^2/g, cumulative pore volume= 4.39 mL/g) [37], was used as catalytic reference system. Pt@C was synthesized as Pt@$L^{1/2}$ (Scheme 1c), contained the same amount of Pt (1.0 wt%) and was featured by the same NPs' size (*i.e.* 1.4 ± 0.4 nm) (Fig. S5). Carbonaceous supports, such

as activated carbon [38], carbon nanotubes [39,40] or carbon nanofibers [41] were successfully used to support Pt NPs employed in the hydrogenation of aromatic nitro compounds. Catalytic blank reactions with $L^{1/2}$ gave no substrate conversion, proving that the catalytic activity of Pt@$L^{1/2}$ is due to the presence of Pt NPs.

From a perusal of the catalytic results shown in Table 1 it can be inferred that: (*i*) Under identical experimental conditions, the catalytic activity of Pt@L^2 was notably higher compared to that of Pt@L^1, regardless of the substrate used (Table 1, entry 3 *vs* 1, entry 8 *vs* 5, entry 14 *vs* 12, entry 18 *vs* 16, entry 22 *vs* 20 and entry 26 *vs* 24). In case of substrates A-C and E, Pt@L^2 showed even higher catalytic conversions than Pt@C (Table 1).

Table 1, here

(*ii*) Regardless of the substrate used, the addition of PEG 5000 (25.0 mg) to Pt@L^1-catalyzed hydrogenation reaction exerted no significant effect on the catalytic activity of the latter (*i.e.* Table 1, entry 2 *vs* 1, entry 6 *vs* 5, entry 13 *vs* 12, entry 17 *vs* 16, entry 21 *vs* 20 and entry 25 *vs* 24). This experimental result corroborated the need of a PEG phase, covalently anchored to sc-PLA, as present in L^2, to improve the catalytic activity of the Pt NPs.

(*iii*) The hydrogenation of substrates A-F (Scheme 2) gave the corresponding aniline and trace amounts of the dehalogenated compound. The chemoselectivity for the corresponding aniline, as shown in Table 1 for catalytic reactions lasting half an hour, was high for all catalysts used (*i.e.* > 99.4%). The dinitro compound F underwent under the same catalytic conditions a selective monohydrogenation, resulting a mixture of 2-chloro-5-nitroaniline and 4-chloro-3-nitroaniline, with a preferred formation of the former (Table 1, entries 24-27). The high chemoselectivity observed for all catalysts was maintained even after complete substrate conversion, as proved by catalytic reactions lasting 1.5 h (Table S3). Prolonged reactions (1.5h) with substrate F (Table S3) gave with

Pt@C complete conversion to 4-Chloro-1,3-diaminobenzene, while Pt@$L^{1/2}$ showed only a partial conversion in the latter dihydrogenated product.

(*iv*) Pt@$L^{1/2}$ proved to be recyclable catalysts, maintaining their performance in terms of catalytic activity and chemoselectivity during at least four consecutive catalytic experiments, showing for Pt@L^2 always higher catalytic activity compared to Pt@L^1 (Table 1, entry 5 *vs* 7 and 8 *vs* 10). The progress of the catalytic hydrogenation reactions was established by carrying out identical catalytic reactions lasting different reaction times, followed by analyzing the catalytic solution upon GC-FID and GC-MS. In Table 2 are reported the catalytic results obtained by a time-dependent hydrogenation of substrate A with Pt@$L^{1/2}$/C.

Table 2, here

Pt@$L^{1/2}$ were separated from solution by centrifugation and decantation in air atmosphere. The resulting solutions were analyzed by ICP-OES, exhibiting a Pt content of 0.04 and 0.46 ppm, which corresponded to 0.16% (Pt@L^1) and 1.8% (Pt@L^2) of the original Pt content. The addition of diethyl ether (2.0 mL) to the catalytic suspension of Pt@L^2, prior to centrifugation, reduced the amount of Pt in solution to 0.08 ppm. This experimental data is in accordance with the slightly higher solubility of L^2 than L^1 in MeOH, due to the MeOH affinity of the PEG.

The recovered catalysts were analyzed by PXRD and HRTEM. The PXRD spectrum of recovered Pt@L^2 (Fig. 5, trace b) proved that the PEG phase recrystallized upon separation from the catalytic solution.

HRTEM micrographs and histograms of Pt@$L^{1/2}$, recovered after the fourth catalytic run (Fig. 6) showed an increase of the Pt NPs size to 2.3 ± 0.4 (Pt@L^1) and 2.1 ± 0.4 nm (Pt@L^2). This latter

particle size was already reached after the first catalytic experiment, as shown for Pt@L^2 (*i.e.* 2.2 ± 0.5 nm) (Fig. 6, middle). We did not observe the presence of Sn NPs in the recovered catalysts by HRTEM, which is in accordance with the neat of stronger reducing agents for Sn(II) reduction [42].

In order to discuss the catalytic performance of Pt@$L^{1/2}$/C during recycling experiments we compiled the most significant data, such as particle size, TOF and selectivity values using substrate B.

Table 3, here

Pt NPs of comparable size (1.4-1.6 nm), supported on $L^{1/2}$ and C, showed under identical experimental conditions different catalytic activities (Table 3) but almost identical chemoselectivity for the corresponding aniline. Hence the support effect on the catalytic activity is evident. Regardless of the nature of the support the NPs' size increased, less in case of the carbon support (Table 3). The covalently attached PEG phase in L^2 exhibited no significant contribution to the stabilization of the NPs' size (Table 3), while its effect on the catalytic activity is clearly shown by comparing the catalytic activities of Pt@L^1 and Pt@L^2 under identical experimental conditions.

Hence the role of the polyether structure of the covalently attached PEG in L^2 may consist in changing the polarity of MeOH, as shown for water [43,44], through hydrogen bond acceptor properties of the PEG oxygen atoms located in close proximity to the supported Pt NPs, creating thus a less polar microenvironment (*i.e.* reducing hydrogen bond interactions between MeOH and the nitro group of the substrate) around the Pt NPs, which might foster the interaction of the aromatic ring of the nitro compounds with the Pt NPs' surface atoms. In fact, the apolar surface of the carbon support is outperformed in most cases by L^2 (Table 1).

The experimental result, that only the corresponding aniline was found in high selectivity (> 99.4%), with the dehalogenated counterpart as the only by-product at different substrate conversions (Tables 2, S3) is a strong hint for a rapid conversion of aromatic nitro compounds on the surface of small Pt NPs to aniline without dissociation of intermediates, which would favor the formation of dimer species such as azoxy- or azobenzene and hydrazine) (Scheme 3) [2,45].

The same sized Pt NPs on different supports (*i.e.* Pt@$L^{1/2}$ *vs* Pt@C) led to the same chemoselectivity of the hydrogenation reaction (Tables 1-3) and on increasing the particle size the chemoselectivity decreased (Table 3), corroborating the size dependents of the chemoselectivity [46]. The only side reaction observed was the hydrodehalogenation reaction, which occurred, as generally accepted, through an electrophilic attack of the cleaved hydrogen on the adsorbed aromatic halide [16,47]. A decrease of the Pt NPs' size increases the electrophilicity of the surface atoms [48,49] depressing the hydrodehalogenation reaction by weakening the electron back donation from Pt NPs to the aromatic ring of the chloroaniline.

4. Conclusions

Pt NPs, generated by the metal vapor synthesis technique and supported onto stereocomplexed PLA without (Pt@L^1) and with a covalently attached PEG phase (Pt@L^2) were successfully applied to hydrogenate aromatic nitro compounds bearing chlorine and reducible functional groups to the corresponding aniline in MeOH under very mild catalytic conditions (*i.e.* 30.0 °C, p(H_2)= 5.0 bar).

The covalently attached PEG phase played a significant role in steering the catalytic activity of the Pt NPs in its close proximity, outperforming not only Pt@L^1 but also with some substartes the reference catalyst (*i.e.* same sized Pt NPs on a high surface carbon support). The observed

chemoselectivity for the corresponding aniline was high with all catalysts studied and mainly determined by the size of the Pt NPs.

Pt@L^2 was completely recyclable by simple centrifugation of the catalytic suspension in air atmosphere, showing comparable catalytic performances in four consecutive catalytic runs.

Acknowledgements

C. E. and C. T. thank MIUR-Italy (FIRB 2010; contract RBFR10BF5V) for financial support.

AppendixA. Supplementary material

Supplementary data associated with this article can be found, in the online version, at http.

References

[1] G. Wegener, M. Brandt, L. Duda, J. Hofmann, B. Klesczewski, D. Koch, R.-J. Kumpf, H. Orzesek, H.-G. Pirkl, C. Six, C. Steinlein, M. Weisbeck, Appl. Catal. A: Gen. 221 (2001) 303.

[2] P. Lara, K. Philippot, Catal. Sci. Technol. 4 (2014) 2445.

[3] E.H. Boymans, P.T. Witte, D. Vogt, Catal. Sci. Technol. 5 (2015) 176.

[4] Z. Rong, W. Du, Y. Wang, L. Lu, Chem. Commun. 46 (2010) 1559.

[5] H. Liu, M. Liang, C. Xiao, N. Zheng, X. Feng, Y. Liu, J. Xie, Y. Wang, J. Mol. Catal. A: Chem. 308 (2009) 79.

[6] M. Lakshmi Kantam, R. Chakravarti, U. Pal, B. Sreedhar, S. Bhargava, Adv. Synth. Catal. 350 (2008) 822.

[7] A. Mori, T. Mizusaki, M. Kawase, T. Maegawa, Y. Monguchi, S. Takao, Y. Takagi, H. Sajiki, Adv. Synth. Catal. 350 (2008) 406.

[8] D. Dutta, D. Kumar Dutta, Appl. Catal. A: Gen. 487 (2014) 158.

[9] S. Zhao, H. Liang, Y. Zhou, Catal. Commun. 8 (2007) 1305.

[10] Y. Chen, C. Wang, H. Liu, J. Qiu, X. Bao, Chem. Commun. (2005) 5298.

[11] K. Shimizu, Y. Miyamoto, A. Satsuma, J. Catal. 270 (2010) 86.

[12] R.V. Jagadeesh, K. Natte, H. Junge, M. Beller, ACS Catal. 5 (2015) 1526.

[13] T. Mitsudome, K. Kaneda, Green Chem. 15 (2013) 2636.

[14] A. Corma, P. Serna, Science 313 (2006) 332.

[15] G. Vilè, N. Almora-Barrios, N. López, J. Pérez-Ramírez, ACS Catal. 5 (2015) 3767.

[16] J. Zhang, Y. Wang, H. Ji, Y. Wei, N. Wu, B. Zuo, Q. Wang, J. Catal. 229 (2005) 114.

[17] M. Liang, X. Wang, H. Liu, H. Liu, Y. Wang, J. Catal. 255 (2008) 335.

[18] X. Wang, M. Liang, H. Liu, Y. Wang, J. Mol. Catal. A: Chem. 273 (2007) 160.

[19] C. Evangelisti, L. A. Aronica, M. Botavina, G. Martra, C. Battocchio, G. Polzonetti, J. Mol. Catal. A: Chem. 366 (2013) 288.

[20] V. Pandarus, R. Ciriminna, F. Béland, M. Pagliaro, Adv. Synth. Catal. 353 (2011) 1306.

[21] F. Cárdenas-Lizana, C. Berguerand, I. Yuranov, L. Kiwi-Minsker, J. Catal. 301 (2013) 103.

[22] A. Noschese, A. Buonerba, P. Canton, S. Milione, C. Capacchione, A. Grassi, J. Catal. 340 (2016) 30.

[23] M. Králik, A. Biffis, J. Mol. Catal. A: Chem. 177 (2001) 113.

[24] K. Xu, Y. Zhang, X. Chen, L. Huang, R. Zhang, J. Huang, Adv. Synth. Catal. 353 (2011) 1260.

[25] M.J. Beier, J.-M. Andanson, A. Baiker, ACS Catal. 2 (2012) 2587.

[26] C.-x. Xiao, H.-z. Wang, X.-d. Mu, Y. Kou, J. Catal. 250 (2007) 25.

[27] H. Cheng, C. Xi, X. Meng, Y. Hao, Y. Yu, F. Zhao, J. Colloid Interface Sci. 336 (2009) 675.

[28] H. Cheng, X. Meng, L. He, W. Lin, F. Zhao, J. Colloid Interface Sci. 415 (2014) 1.

[29] E. Colacino, J. Martinez, F. Lamaty, L.S. Patrikeeva, L.L. Khemchyan, V.P. Ananikov, I.P. Beletskaya, Coord. Chem. Rev. 256 (2012) 2893.

[30] G. Petrucci, W. Oberhauser, M. Bartoli, G. Giachi, M. Frediani, E. Passaglia, L. Capozzoli, L. Rosi, Appl. Catal. A: Gen. 469 (2014) 132.

[31] W. Oberhauser, C. Evangelisti, R.P. Jumde, G. Petrucci, M. Bartoli, M. Frediani, M. Mannini, L. Capozzoli, E. Passaglia, L. Rosi, J. Catal. 330 (2015) 187.

[32] S.N. Sidorov, L.M. Bronstein, P.M.Valetsky, J. Hartmann, H. Cölfen, H. Schnablegger, M. Antonietti, J. Colloid Interface Sci. 212 (1999) 197.

[33] H.R. Kricheldorf, I. Kreiser-Saunders, C. Boettcher, Polymer 36 (1995) 1253.

[34] G. Vitulli, C. Evangelisti, A.M. Caporusso, P. Pertici, N. Panziera, S. Bertozzi, P. Salvadori, in: B. Corain, G. Schmid, N. Toshima (Eds.), Metal Nanoclusters in Catalysis and Material Science: The issue of Size Control, Elsevier, Amsterdam, 2008, pp. 437-451.

[35] A. Borodziński, M. Bonarowska, Langmuir 13 (1997) 5613.

[36] J.R. Murdoch, G.L. Loomis, US patent 4719246A.

[37] W. Oberhauser, C. Evangelisti, R.P. Jumde, R. Psaro, F. Vizza, M. Bevilacqua, J. Filippi, B.F. Machado, P. Serp, J. Catal. 325 (2015) 111.

[38] M. Jianzhong, Y. Xinhuan, G. Huizi, J. Lingchao, Chin. J. Catal 30 (2009) 182.

[39] L. Jiang, H. Gu, X. Xu, X. Yan, J. Mol. Catal. A: Chem. 310 (2009) 144.

[40] Z. Sun, Y. Zhao, Y. Xie, R. Tao, H. Zhang, C. Huang, Z. Liu, Green Chem. 12 (2010) 1007.

[41] M. Takasaki, Y. Motoyama, K. Higashi, S.-H. Yoon, I. Mochida, H. Nagashima, Org. Lett. 10 (2008) 1601.

[42] D.V. Goia, E. Matijević, New J. Chem. (1998) 1203.

[43] J. Chen, S.K. Spear, J.G. Huddleston, R.D. Rogers, Green Chem. 7 (2005) 64.

[44] G. Karlström, J. Phys. Chem. 89 (1985) 4962.

[45] H.-U. Blaser, H. Steiner, M. Studer, ChemCatChem 1 (2009) 210.

[46] A. Corma, P. Serna, P. Concepción, J.J. Calvino, J. Am. Chem. Soc. 130 (2008) 8748.

[47] C. Menini, C. Park, E.-J. Shin, G. Tavoularis, M.A. Keane, Catal. Today 62 (2000) 355.

[48] B. Coq, G. Ferrat, F. Figueras, J. Catal. 101 (1986) 434.

[49] B. Coq, A. Tijani, F. Figuéras, J. Mol. Catal. 68 (1991) 331.

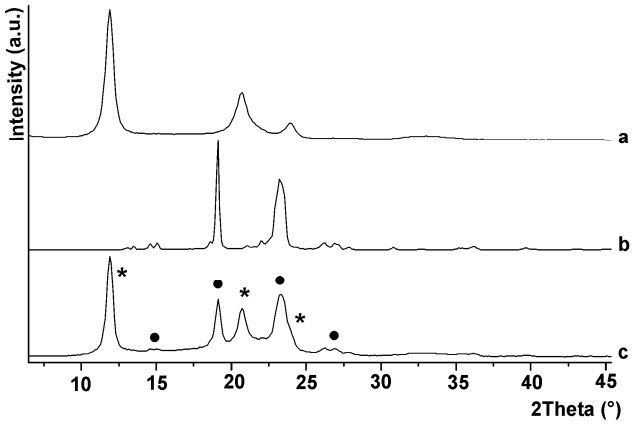

Fig. 1. PXRD spectra of L^1 (a), PEG (b) and L^2 (c). Asterisks and full circles denote Bragg reflexes assigned to sc-PLA and PEG, respectively.

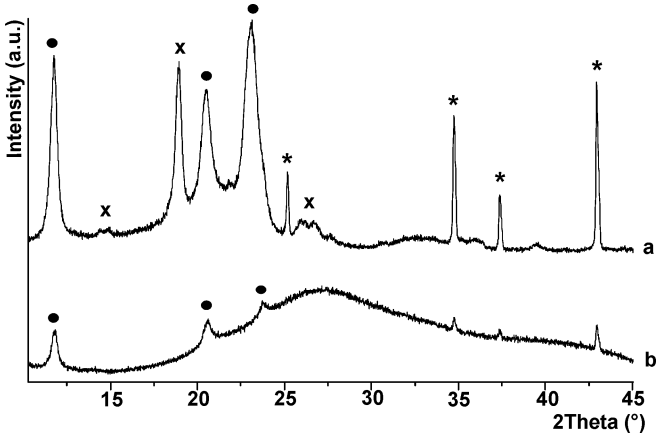

Fig. 2. PXRD spectra acquired at room temperature of L^2: as-synthesized (a) and as MeOH suspension (b). Asterisks denote reflexes stemming from sample holder (Al_2O_3), while full circles and x refer to characteristic Bragg reflexes of sc-PLA and PEG, respectively.

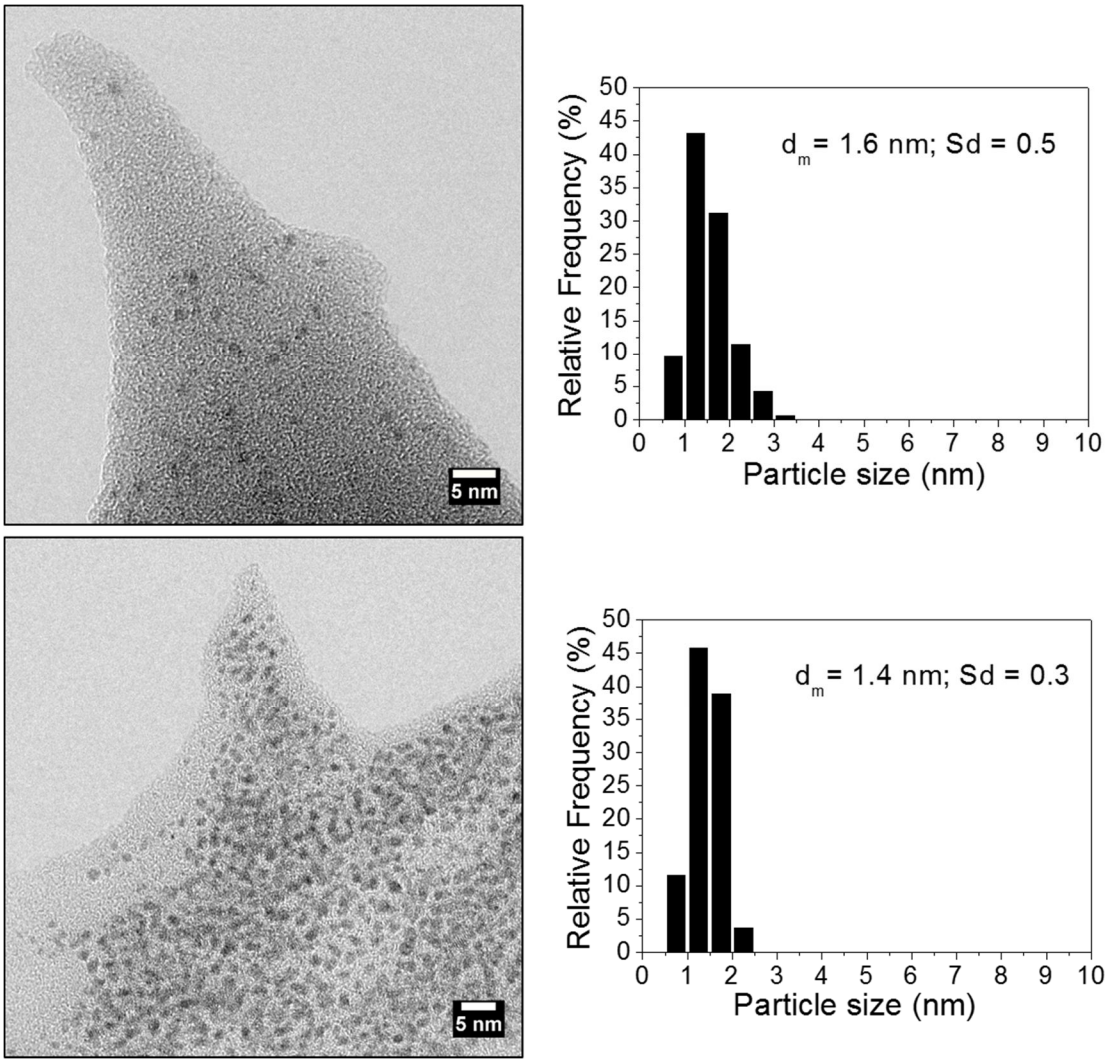

Fig. 3. HRTEM micrographs and histograms for Pt@L^1 (top) and Pt@L^2 (bottom).

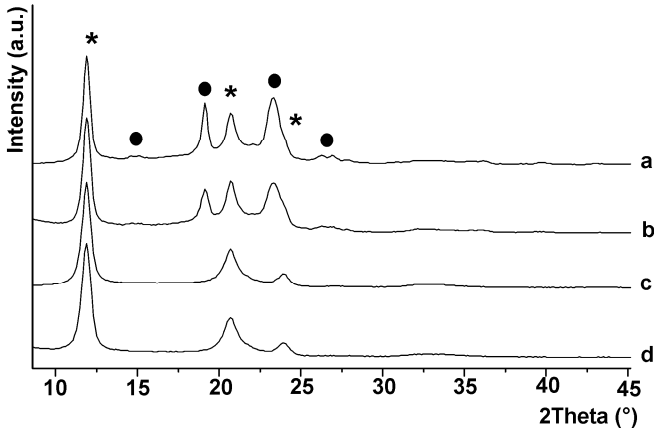

Fig. 4. PXRD spectra of L^2 (a), Pt@L^2 (b), L^1 (c) and Pt@L^1 (d).

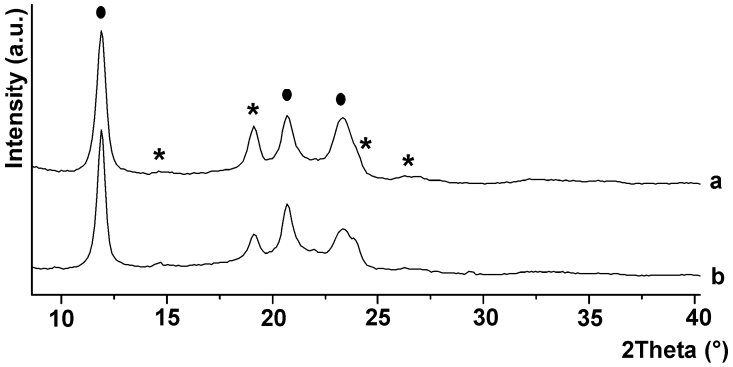

Fig. 5. PXRD spectra of Pt@L^2: as-synthesized (a) and after recovering (b). Full circles and asterisks denote Bragg reflexes assigned to sc-PLA and PEG, respectively.

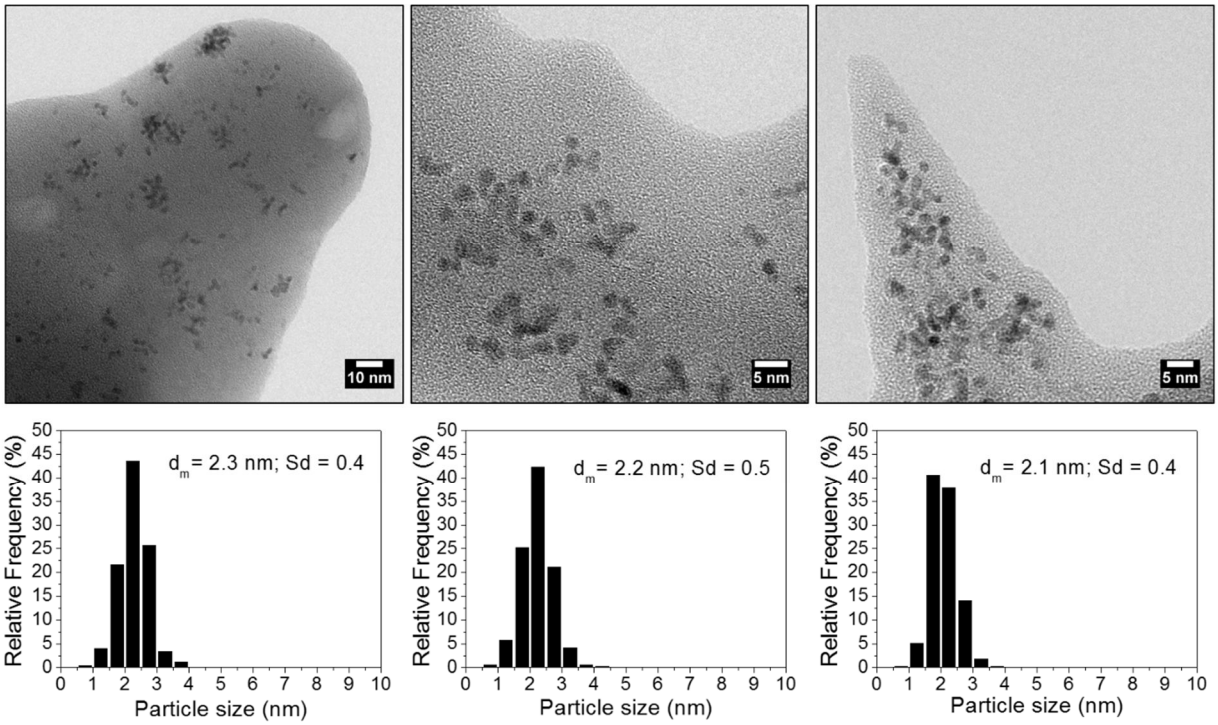

Fig. 6. HRTEM micrographs and histograms for recovered catalysts: Pt@L^1 after the fourth catalytic run (left); Pt@L^2 after the first (middle) and fourth catalytic run (right).

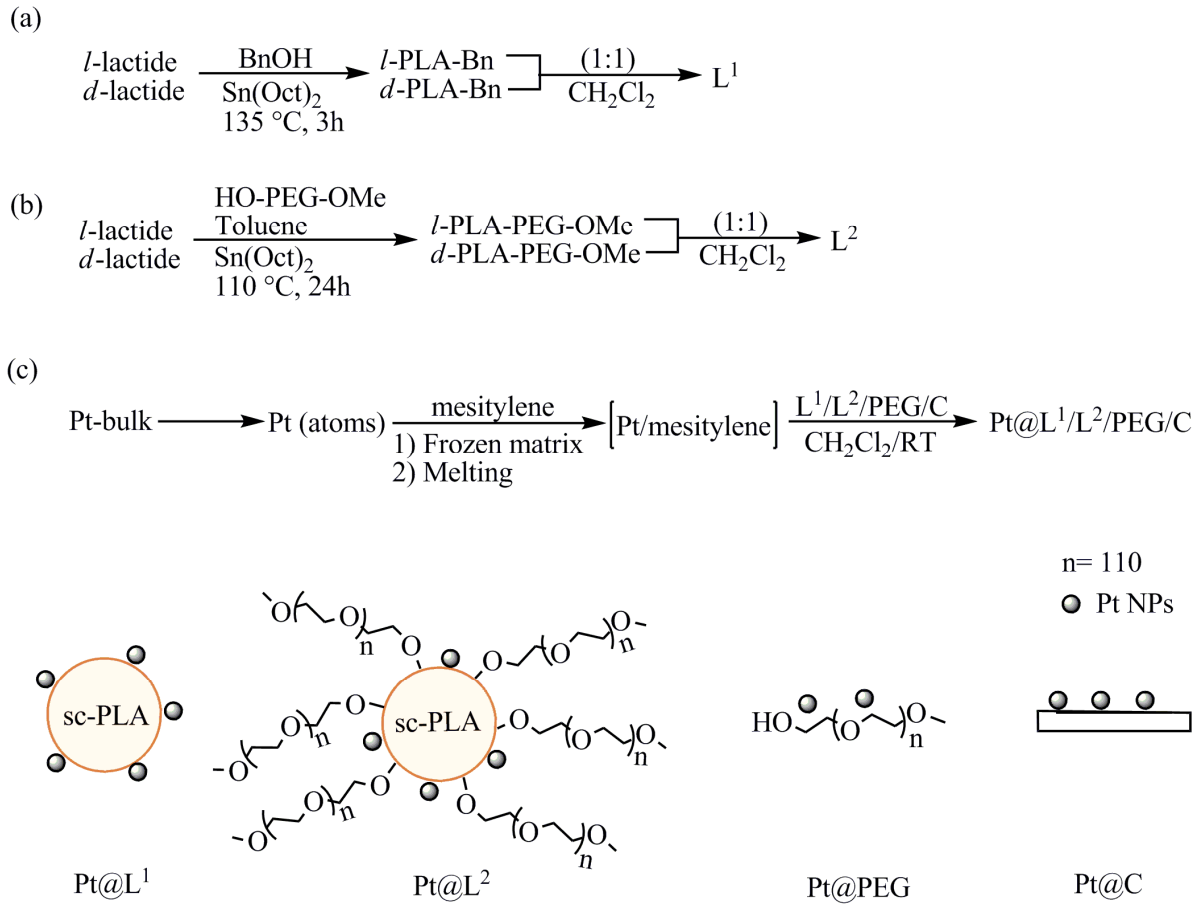

Scheme 1. Synthesis of sc-PLA, supported Pt NPs (a-c) and pictorial presentation of Pt NPs supported onto $L^{1/2}$, PEG and carbon (C).

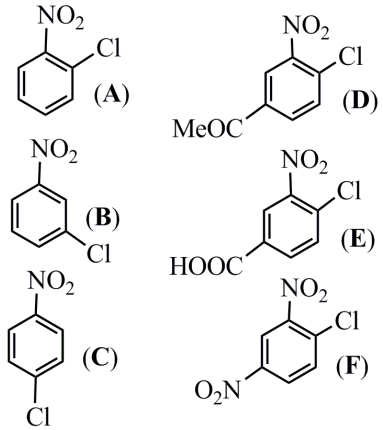

Scheme 2. Substrates used for the catalytic screening.

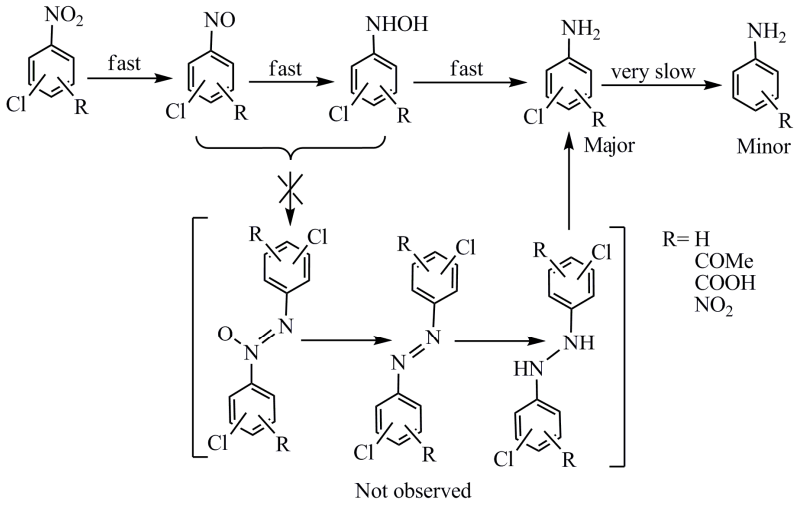

Scheme 3. Proposed reaction mechanism for Pt@$L^{1/2}$/C-mediated aromatic nitrocompound hydrogenation reactions.

Table 1
Hydrogenation of selected aromatic nitrocompounds by supported Pt-NPs.

Entry[a]	Catalyst	Substrate	mmol(Substr.)/(Substr./ $Pt_{surface}$ molar ratio)	Conv.(%) [TOF (h^{-1})]	Sel.(%)[b]
1	Pt@L[1]	A	4.077/5679	42.1 [4782]	99.8
2[c]	Pt@L[1]			43.3 [4918]	99.8
3	Pt@L[2]		4.077/5129	63.5 [6514]	99.6
4	Pt@C		4.0775129	55.6 [5704]	99.5
5	Pt@L[1]	B	4.077/5679	43.6 [4952]	99.8
6[c]	Pt@L[1]			45.0 [5111]	99.8
7[d]	Pt@L[1]			31.8 [4600]	99.5
8	Pt@L[2]		4.077/5129	69.8 [7161]	99.8
9[e]	Pt@L[2]			53.9 [7080]	99.6
10[d]	Pt@L[2]			53.0 [7010]	99.5
11	Pt@C		4.077/5129	51.7 [5304]	99.9
12	Pt@L[1]	C	4.077/5679	24.4 [2771]	99.7
13[c]	Pt@L[1]			26.9 [3055]	99.8
14	Pt@L[2]		4.077/5129	49.5 [5078]	99.7
15	Pt@C		4.077/5129	42.6 [4370]	99.8
16	Pt@L[1]	D	2.039/2840	72.3 [4107]	99.9
17[c]	Pt@L[1]			73.0 [4147]	99.8
18	Pt@L[2]		2.039/2565	83.7 [4294]	99.9
19	Pt@C		2.039/2565	95.8 [4915]	99.9
20	Pt@L[1]	E	2.039/2840	58.8 [3340]	99.9
21[c]	Pt@L[1]			60.1 [3414]	99.8
22	Pt@L[2]		2.039/2565	94.0 [4823]	99.9
23	Pt@C		2.039/2565	80.6 [4135]	99.9
24	Pt@L[1]	F	2.039/2840	54.4 [3090]	99.9 (4.5:1)[f]
25[c]	Pt@L[1]			57.0 [3238]	99.9 (4.4:1)[f]
26	Pt@L[2]		2.039/2565	70.9 [3638]	99.8(5.6:1)[f]
27	Pt@C		2.039/2565	94.7 [4859]	99.9 (7.2:1)[f]

[a] Catalytic conditions: Catalyst (25.0 mg, 1.282 μmol of Pt), MeOH (10.0 mL), T= 30.0 °C, $p(H_2)$= 5.0 bar, t= 0.5h.
[b] Selectivity referred to the corresponding aniline compound.
[c] Addition of PEG (25.0 mg).
[d] Fourth run.
[e] Second run.
[f] Molar ratio between 2-chloro-5-nitroaniline and 4-chloro-3-nitroaniline.

Table 2
Time-dependent hydrogenation of substrate A with Pt@$L^{1/2}$/C.

Entry[a]	Catalyst	Substr./$Pt_{surface}$ molar ratio	t(h)	Conv.(%) [TOF (h^{-1})]	Sel.(%)[b]
1	Pt@L^1	5679	0.25	22.0 [4997]	99.7
2	Pt@L^1	5679	0.5	43.3 [4918]	99.8
3	Pt@L^1	5679	1.0	82.0 [4657]	99.8
4	Pt@L^2	5129	0.25	30.2 [6155]	99.8
5	Pt@L^2	5129	0.5	58.5 [6002]	99.6
6	Pt@L^2	5129	1.0	100.0 [n.d.]	99.7
7	Pt@C	5129	0.25	28.0 [5745]	99.6
8	Pt@C	5129	0.5	55.6 [5704]	99.5
9	Pt@C	5129	1.0	100.0 [n.d.]	99.5

[a] Catalytic conditions: Catalyst (25.0 mg, 1.282 μmol of Pt), substrate A (4.077 mmol), MeOH (10.0 mL), T= 30.0 °C, p(H_2)= 5.0 bar.
[b] Selectivity referred to the corresponding aniline compound.

Table 3
Recycling experiments with Pt@$L^{1/2}$/C.

Catalyst[a]	Substr./$Pt_{surface}$ molar ratio $1^{st}/4^{th}$ run	Particle size (nm) (as-synthesized)	Particle size (nm) after 4^{th} run	TOF (h^{-1})/ Sel.(%)[b] 1^{st} run	TOF (h^{-1})/ Sel.(%)[b] 4^{th} run
Pt@L^1	5679/7227	1.6 ± 0.5	2.3 ± 0.4	4952/99.8	4600/99.5
Pt@L^2	5129/6625	1.4 ± 0.3	2.1 ± 0.4	7161/99.8	7010/99.5
Pt@C	5129/5889	1.4 ± 0.4	1.8 ± 0.4	5304/99.9	5002/99.7

[a] Catalytic conditions: Catalyst (25.0 mg, 1.282 μmol of Pt), substrate B (4.077 mmol), MeOH (10.0 mL), T= 30.0 °C, p(H_2)= 5.0 bar, t= 0.5h.
[b] Selectivity referred to the corresponding aniline.